J|A|C|S
ARTICLES
Published on Web 08/11/2006

(^{t}Bu$_2$MeSi)$_2$Sn=Sn(SiMe^{t}Bu$_2$)$_2$: A Distannene with a >Sn=Sn< Double Bond That Is Stable Both in the Solid State and in Solution

Vladimir Ya. Lee,[†] Tomohide Fukawa,[†] Masaaki Nakamoto,[†] Akira Sekiguchi,*[,†] Boris L. Tumanskii,[‡] Miriam Karni,[‡] and Yitzhak Apeloig[‡]

Contribution from Department of Chemistry,Graduate School of Pure and Applied Sciences, University of Tsukuba, Tsukuba, Ibaraki 305-8571, Japan, and Department of Chemistry, Technion-Israel Institute of Technology, Haifa 32000, Israel

Received May 12, 2006; E-mail: sekiguch@staff.chem.tsukuba.ac.jp

Abstract: (^{t}Bu$_2$MeSi)$_2$Sn=Sn(SiMe^{t}Bu$_2$)$_2$ **1**, prepared by the reaction of ^{t}Bu$_2$MeSiNa with SnCl$_2$-diox in THF and isolated as dark-green crystals, represents the first example of acyclic distannene with a Sn=Sn double bond that is stable both in the crystalline form and in solution. This was proved by the crystal and NMR spectral data of **1**. Distannene **1** has these peculiar structural features: a shortest among all acyclic distannenes Sn=Sn double bond of 2.6683(10) Å, a nearly planar geometry around both Sn atoms, and a highly twisted Sn=Sn double bond. The reactions of **1** toward carbon tetrachloride and phenylacetylene also correspond to the reactivity anticipated for the Sn=Sn double bond. The one-electron reduction of **1** with potassium produced the distannene anion radical, the heavy analogue of alkene ion radicals, for which the particular crystal structure and low-temperature EPR behavior are also discussed.

Introduction

The distannenes, that is, the compounds featuring Sn=Sn double bonds, have been known for nearly 30 years, since the first stable alkene analogue of group 14 elements heavier than carbon was reported by Lappert in 1976.[1] This breakthrough discovery of Dis$_2$Sn=SnDis$_2$ (Dis = CH(SiMe$_3$)$_2$) has, in fact, opened the door to a broad avenue of heavy alkene analogues of group 14 elements, one of the most compelling topics of modern organometallic chemistry. Since then the chemistry of heavy alkene analogues, known also as dimetallaalkenes or dimetallenes, has been greatly developed in all aspects: synthetic, structural, reactivity. To date, many representatives of both homonuclear (disilenes, digermenes, distannenes, diplumbenes) and heteronuclear (silenes, germenes, stannenes, silagermenes, silastannenes, germastannenes) heavy alkene analogues have been synthesized and, in a majority of cases, structurally characterized.[2] The striking progress in this field is reflected in the number of recent reviews devoted to this topic.[3] Very recently, unsaturated small (three- and four-membered) cyclic compounds composed of heavier group 14 elements also became synthetically accessible as a new class of cyclic heavy alkene analogues.[4]

It is now well-known and widely accepted that the nature of the double bond between the heavier group 14 elements is significantly different from that of the classical carbon−carbon double bond in organic chemistry.[3a] The progressively increasing difference between the size and energy of s- and p-orbitals descending group 14 makes them more reluctant for sp^2-type hybridization in its classical sense, particularly for the heaviest

[†] University of Tsukuba.
[‡] Technion-Israel Institute of Technology.

(1) (a) Goldberg, D. E.; Harris, D. H.; Lappert, M. F.; Thomas, K. M. *J. Chem. Soc., Chem. Commun.* **1976**, 261. (b) Goldberg, D. E.; Hitchcock, P. B.; Lappert, M. F.; Thomas, K. M.; Thorne, A. J.; Fjeldberg, T.; Haaland, A.; Schilling, B. E. R. *J. Chem. Soc., Dalton Trans.* **1986**, 2387.

(2) Only the first stable representatives for each class of the heavy alkenes are given below. Disilene: (a) West, R.; Fink. M. F.; Michl, J. *Science* **1981**, *214*, 1343. Digermene: (b) Hitchcock, P. B.; Lappert, M. F.; Miles, S. J.; Thorne, A. J. *J. Chem. Soc., Chem. Commun.* **1984**, 480 and ref 1b. Distannene: (c) see ref 1. Diplumbene: (d) Stürmann, M.; Saak, W.; Marsmann, H.; Weidenbruch, M. *Angew. Chem., Int. Ed.* **1999**, *38*, 187. Silene: (e) Brook, A. G.; Abdesaken, F.; Gutekunst, B.; Gutekunst, G.; Kallury, R. K. M. R. *J. Chem. Soc., Chem. Commun.* **1981**, 191. Germenes: (f) Couret, C.; Escudié, J.; Satge, J.; Lazraq, M. *J. Am. Chem. Soc.* **1987**, *109*, 4411 and (g) Meyer, H.; Baum, G.; Massa, W.; Berndt, A. *Angew. Chem., Int. Ed. Engl.* **1987**, *21*, 221. Stannene: (h) Meyer, H.; Baum, G.; Massa, W.; Berger, S.; Berndt, A. *Angew. Chem., Int. Ed. Engl.* **1987**, *26*, 546. Silagermene: (i) Lee, V. Ya.; Ichinohe, M.; Sekiguchi, A.; Takagi, N.; Nagase, S. *J. Am. Chem. Soc.* **2000**, *122*, 9034. Silastannene: (j) Sekiguchi, A.; Izumi, R.; Lee, V. Ya.; Ichinohe, M. *J. Am. Chem. Soc.* **2002**, *124*, 14822. Germastannenes: (k) Schafer, A.; Saak, W.; Weidenbruch, M. *Organometallics* **2003**, *22*, 215. (l) Sekiguchi, A.; Izumi, R.; Lee, V. Ya.; Ichinohe, M. *Organometallics* **2003**, *22*, 1483 and (m) Lee, V. Ya.; Takanashi, K.; Ichinohe, M.; Sekiguchi, A. *J. Am. Chem. Soc.* **2003**, *125*, 6012.

(3) (a) Power, P. P. *Chem. Rev.* **1999**, *99*, 3463. (b) Weidenbruch, M. *Eur. J. Inorg. Chem.* **1999**, 373. (c) Escudié, J.; Ranaivonjatovo, H. *Adv. Organomet. Chem.* **1999**, *44*, 113. (d) Kira, M.; Iwamoto, T. *J. Organomet. Chem.* **2000**, *611*, 236. (e) Weidenbruch, M. In *The Chemistry of Organic Silicon Compounds*; Rappoport, Z., Apeloig, Y., Eds.; Wiley: Chichester, U.K., 2001; Vol. 3, Chapter 5. (f) Klinkhammer, K. In *The Chemistry of Organic Germanium, Tin and Lead Compounds*; Rappoport, Z., Ed.; Wiley: Chichester, U.K., 2002; Vol. 2, Part 1, Chapter 4. (g) Tokitoh, N.; Okazaki, R. In *The Chemistry of Organic Germanium, Tin and Lead Compounds*; Rappoport, Z., Ed.; Wiley: Chichester, U.K., 2002; Vol. 2, Part 1, Chapter 13. (h) Weidenbruch, M. *Organometallics*, **2003**, *22*, 4348. (i) Lee V. Ya; Sekiguchi, A. *Organometallics*, **2004**, *23*, 2822.

(4) Reviews on the three-membered ring unsaturated compounds of heavier group 14 elements (heavy cyclopropenes): (a) Lee, V. Ya; Sekiguchi, A. In *The Chemistry of Organic Germanium, Tin and Lead Compounds*; Rappoport, Z., Ed.; Wiley: Chichester, U.K., 2002; Vol. 2, Part 1, Chapter 14. (b) Sekiguchi, A.; Lee V. Ya. *Chem. Rev.* **2003**, *103*, 1429. (c) Sekiguchi, A.; Lee, V. Ya. In *Organosilicon Chemistry V: From Molecules to Materials*; Auner, N., Weis, J., Eds.; Wiley-VCH: Weinheim, Germany, 2003; p 92.

Scheme 1

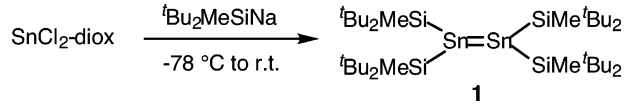

1

group 14 elements (Sn, Pb). In other words, on going down group 14 from C to Pb, there is an apparent and strong tendency for a steady increase in the lone-pair character versus double-bond character of the elements forming the double bond.[3a] This finally results in the highly pronounced pyramidalization of the doubly bonded elements, stretching of the double bond, and, consequently, decrease in its strength.

It is, therefore, not surprising that typical disilenes and digermenes maintain their relatively short and strong Si═Si and Ge═Ge double bonds both in the crystalline form and in solution.[3a,f,g] In marked contrast, all distannenes and diplumbenes known to date possess rather long Sn═Sn and Pb═Pb double bonds, which are very close to (or even longer than) the Sn—Sn and Pb—Pb single bonds.[3a,f,g] Accordingly, the heaviest alkenes of the type >E═E< (E = Sn, Pb) dissociate in solution into a pair of corresponding heavy carbene analogues, >E**:**. In fact, all distannenes known to date, even those structurally characterized in the crystalline form as doubly bonded species, undergo unavoidable double bond breaking in solution to produce the corresponding stannylenes.[3f,g] This was clearly demonstrated by their spectral (NMR, UV) and chemical properties in solution corresponding to the behavior of stannylenes rather than real distannenes. As theoretical support, recent ELF and AIM calculations attributed the weakness of the Sn═Sn double bond to the lower attraction and decreased localization of the valence shell electrons into the bonding region because of the larger size and lower electronegativity of the tin atoms.[5] In the latest review dealing with distannenes, it was pointed out: "A distannene which does not dissociate into stannylenes in solution is still unknown."[3g] Now this situation is remedied because of our synthesis of tetrakis(di-*tert*-butylmethylsilyl)distannene, the first compound featuring a Sn═Sn double bond that is stable both in the solid state and in solution.[6] In this paper we wish to report a full account of the synthesis, spectral and structural elucidation, and specific reactivity of this distannene, as well as the structure of its reduction product, the distannene anion radical.

Results and Discussion

Synthesis of Tetrakis(di-*tert*-butylmethylsilyl)distannene 1. Tetrakis(di-*tert*-butyl-methylsilyl)distannene **1** was synthesized by the straightforward reaction of $SnCl_2$-diox with 2.5 equiv of $^tBu_2MeSiNa$ in THF at −78 °C and was isolated by recrystallization from hexane as dark-green crystals in 43% yield (Scheme 1).

It is interesting that the reaction of the same compounds previously reported by us carried out in diethyl ether instead of THF resulted in the formation of the tris(di-*tert*-butylmethylsilyl)stannyl radical ($(^tBu_2MeSi)_3Sn$·**2**[7] instead of distannene **1**. Definitely, such a dramatic difference in the reaction course should be ascribed to the different coordinating abilities of THF vs diethyl ether.

The crystal (X-ray) and spectral (^{119}Sn NMR, UV) characteristics of distannene **1** are particularly important for the discussion of its structure both in the solid state and in solution.

Crystal Structure of 1. The crystal structure of **1** was determined by X-ray crystallographic analysis (Figure 1, Table 1), which revealed several rather unusual structural features. First: the Sn═Sn double bond is very short, 2.6683(10) Å, which should be recognized as the shortest among all structurally characterized stable distannenes reported to date[3a,f,g,8] (Table 2) (the calculated value of the Sn═Sn double bond in the model $(Me_3Si)_2Sn═Sn(SiMe_3)_2$ distannene is 2.6805 Å).[9] This value is nearly 5% shorter than the average value of the Sn—Sn single bond (2.81 Å).[10] In light of the above-mentioned inherent weakness and stretching of Sn═Sn double bonds (see Introduction), the rather short and strong Sn═Sn double bond in distannene **1** is particularly amazing. Indeed, such a phenomenon should originate from the electronic influence of the four σ-donating silyl substituents, because it is well-known that the electropositive groups effectively strengthen the π-bonds between the heavier group 14 elements, whereas electronegative groups have the opposite effect.[3a]

The second structural characteristic worthy of mention is the nonpyramidal geometry around the Sn═Sn double bond: *trans*-bend angle = 1.22(5)°, the sum of the bond angles around the tricoordinate tin atoms = 359.98°. This is the first example of a distannene with a nonpyramidal Sn═Sn skeleton (Table 2).[3f] Such an unusual geometry for the Sn═Sn double bond (together with its shortening) closely resembles the structural properties of alkenes (typically, planar and short C═C double bond), in marked contrast to all other structurally characterized distannenes having a highly pronounced degree of pyramidalization at the Sn═Sn double bond (*trans*-bend angles range from 21.4 to 64.4°).[3a,f,g,8] Such planarization of the double bond in **1** should also be ascribed to the electropositive influence of the silyl substituents.

However, such a great shortening of the Sn═Sn double bond is associated with a significant repulsion between the four highly sterically demanding $^tBu_2MeSi$ substituents, which in turn results in the significant twisting of the Sn═Sn double bond (twisting angle of 44.62(7)°). In effect, distannene **1** has a rather unusual combination of the structural characteristics of the Sn═Sn bonds: it is short, nonpyramidal, and highly twisted (Table 2). It should be mentioned that the combination of such features is rather unusual in the structural chemistry of distannenes. Two bonding models for the double bonds between group 14 elements are now commonly accepted (Scheme 2).[1−4] The first

(5) Malcolm, N. O. J.; Gillespie, R. J.; Popelier, P. L. A. *J. Chem. Soc., Dalton Trans.* **2002**, 3333.
(6) Fukawa, T.; Lee, V. Ya.; Nakamoto, M.; Sekiguchi, A. *J. Am. Chem. Soc.* **2004**, *126*, 11758.
(7) Sekiguchi, A.; Fukawa, T.; Lee, V. Ya.; Nakamoto, M. *J. Am. Chem. Soc.* **2003**, *125*, 9250.
(8) Structurally characterized acyclic distannenes: (a) see ref 1. (b) Klinkhammer, K. W.; Niemeyer, M.; Klett, J. *Chem.—Eur. J.* **1999**, *5*, 2531. (c) Sturmann, M.; Saak, W.; Klinkhammer, K. W.; Weidenbruch, M. *Z. Anorg. Allg. Chem.* **1999**, *625*, 1955. (d) Klinkhammer, K. W.; Schwarz, W. *Angew. Chem., Int. Ed. Engl.* **1995**, *34*, 1334. (e) Klinkhammer, K. W.; Fassler, T. F.; Grutzmacher, H. *Angew. Chem., Int. Ed.* **1998**, *37*, 124.
(9) The theoretical calculations were performed with the GAUSSIAN program package at the B3LYP/6-31G(d) level for H, C, Si and LANL2DZd level for Sn atoms. Frisch, M. J. et al. *Gaussian 98* (revision A.11) and *Gaussian 03* (revision B.05); Gaussian, Inc.: Pittsburgh, PA, 2001. For the B3LYP method: (a) Stephens, P. J.; Devlin, F.; Chabalowski, C. F.; Frisch, M. J. *J. Phys. Chem.* **1994**, *98*, 11623. (b) Hertwig, R. H.; Koch, W. *Chem. Phys. Lett.* **1997**, *268*, 345. (c) Becke, A. D. *J. Chem. Phys.* **1993**, *98*, 5648. (d) Becke, A. D. *Phys. Rev. A* **1988**, *38*, 3098. (e) Lee, C.; Yang, W.; Parr, R. G. *Phys. Rev. B* **1988**, *37*, 785.
(10) Mackay, K. M. In *The Chemistry of Organic Germanium, Tin, and Lead Compounds*; Patai, S., Ed.; Wiley: Chichester, U.K., 1995; Chapter 2.

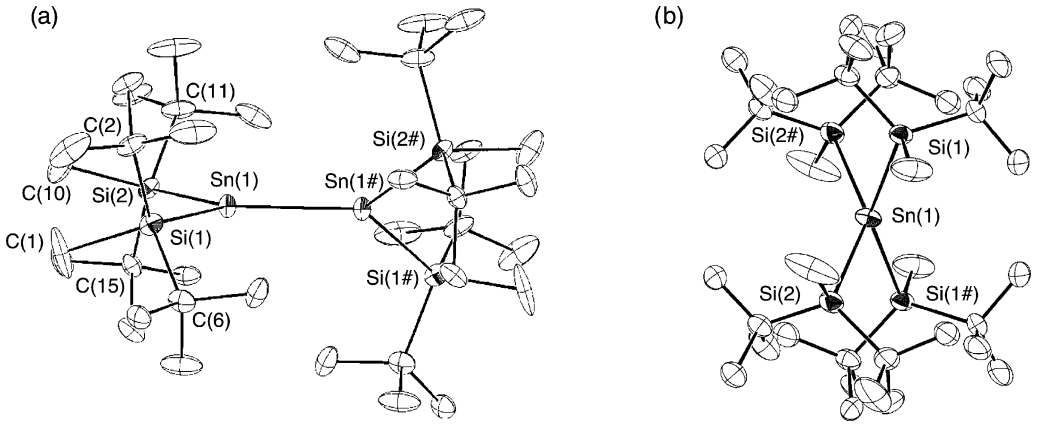

Figure 1. Crystal structure of **1** (ORTEP plot; thermal ellipsoids are shown at the 30% probability; hydrogen atoms are omitted): (a) side view; (b) view along the Sn−Sn bond.

Table 1. Selected Bond Lengths (Å) and Angles (deg) of **1**[a]

Sn(1)−Sn(1#)	2.6683(10)	Sn(1#)−Sn(1)−Si(1)	124.21(7)
Sn(1)−Si(1)	2.631(2)	Sn(1#)−Sn(1)−Si(2)	126.50(5)
Sn(1)−Si(2)	2.630(2)	Si(1)−Sn(1)−Si(2)	109.27(8)
Si(1)−C(1)	1.954(10)	Sn(1)−Si(1)−C(1)	105.6(3)
Si(1)−C(2)	1.904(9)	Sn(1)−Si(1)−C(2)	115.8(3)
Si(1)−C(6)	1.872(10)	Sn(1)−Si(1)−C(6)	109.2(2)
Si(2)−C(10)	1.915(10)	Sn(1)−Si(2)−C(10)	104.3(3)
Si(2)−C(11)	1.897(10)	Sn(1)−Si(2)−C(11)	108.6(4)
Si(2)−C(15)	1.898(9)	Sn(1)−Si(2)−C(15)	116.8(3)

[a] Atomic numbers are given in Figure 1. Standard deviations are in parentheses.

one is applicable to alkenes as formal carbene dimers. Because typical carbenes have either a triplet ground state, $^3B_1$, or a small singlet−triplet energy separation,[11] the formation of the C═C double bond is considered to be a result of interaction between the two triplet carbenes: $\sigma^1-\sigma^1$ (σ-bond) and $p_\pi^1-p_\pi^1$ (π-bond) to form a classical strong covalent double bond with a planar geometry around it (Scheme 2, mode **A**). Another bonding model is employed for the description of the double bond between the heavier group 14 elements. Because all experimentally known heavy carbene analogues (except for (^{t}Bu$_3$Si)$_2$Si**:**[12]) possess a singlet ground state, $^1A_1$, with largely different (by both size and energy) s- and p-orbitals,[13] the interaction between them to form a double bond is not possible in the classical mode, but rather by the double donor−acceptor interaction between the doubly occupied σ-orbitals and empty p_π-orbitals (σ^2-p_π) of the two singlet carbene analogues to form a weak dative E═E bond with the characteristic *trans*-bending of substituents (Scheme 2, mode **B**).

It is apparent that in the particular case of distannene **1** (short, nonpyramidal, and twisted Sn═Sn double bond) one cannot adequately describe the bonding situation using either of the two models discussed above (Scheme 2, modes **A** and **B**). Such an unusual bonding motif in **1** can alternatively be explained as a result of out-of-plane (because of the high steric hindrances due to the bulky silyl substituents) interaction of the two triplet stannylenes (^{t}Bu$_2$MeSi)$_2$Sn**:** ($\sigma^1-\sigma^1$ and $p_\pi^1-p_\pi^1$) resulting in the formation of a nonpyramidal but a highly twisted Sn═Sn double bond (Scheme 2, mode **C**). Indeed, the triplet state of (^{t}Bu$_2$MeSi)$_2$Sn**:** might be easily accessible due to its relatively small singlet−triplet energy gap, $\Delta E_{S-T} = 8.5$ kcal/mol, in favor of the singlet state calculated at the B3LYP/SDD[14] level of theory (however, this value may be overestimated by ca. 2−4 kcal/mol).[15] The significant decrease in the ΔE_{S-T} value for (^{t}Bu$_2$MeSi)$_2$Sn**:** relative to that of Me$_2$Sn**:** (29.5 kcal/mol) can be definitely attributed to the electronic effect of the electropositive silyl substituents and to their large steric bulk, which widens the Si−Sn−Si bond angle from 96.7° in Me$_2$Sn**:** to 109.6° in (^{t}Bu$_2$MeSi)$_2$Sn**:**. This trend is quite similar to the influence of substituents on the ΔE_{S-T} value of silylenes R$_2$Si**:**, in which the electropositive and voluminous silyl groups R also widen the R−Si−R bond angle, thus decreasing ΔE_{S-T} values. Such significantly smaller ΔE_{S-T} values for bulky silyl-substituted silylenes make the singlet−triplet promotion accessible,[16] and the multiplicity order may even be reversed, as was found experimentally for (^{t}Bu$_3$Si)$_2$Si**:**, which has a triplet ground state.[12] As one can expect, when the size of the substituents R in stannylenes R$_2$Sn**:** is successively decreased and the electronegativity of the substituents is increased, the ΔE_{S-T} value progressively increases; namely, for R = ^{t}Bu$_2$MeSi, Me$_3$Si, H$_3$Si, H, and Me, the calculated ΔE_{S-T} values are 8.5, 10.3, 18.0, 26.5, and 29.2 kcal/mol, respectively, at the B3LYP/SDD level (earlier *ab initio* calculations at MCSCF and CCSD(T) levels predicted ΔE_{S-T} values of 22.7 and 27.9 kcal/mol for H$_2$Sn**:**[17] and Me$_2$Sn**:**[18] stannylenes, respectively).

^{119}Sn NMR Spectrum of 1. In solution, distannene **1** expectedly exhibited very simple NMR spectra in accord with its symmetrical composition. Most essential for discussion of the structure of **1** is its ^{119}Sn NMR spectrum measured in benzene-d_6, which revealed a single resonance at +630.7 ppm. Such a chemical shift lies in the region expected for the sp^2-Sn atoms in distannene, we can compare it with the only two

(11) (a) Kirmse, W. *Carbene Chemistry*, 2nd ed.; Academic Press: New York, USA, 1971. (b) Moss, R. A.; Jones, M., Jr. *Carbenes*; Wiley: Chichester, U.K., 1975; Vol. 2. (c) Bourissou, D.; Guerret, O.; Gabbai, F.; Bertrand, G. *Chem. Rev.* **2000**, *100*, 39.
(12) Sekiguchi, A.; Tanaka, T.; Ichinohe, M.; Akiyama, K.; Tero-Kubota, S. *J. Am. Chem. Soc.* **2003**, *125*, 4962.
(13) (a) Neumann, W. P. *Chem. Rev.* **1991**, *91*, 311. (b) Tokitoh, N.; Okazaki, R. *Coord. Chem. Rev.* **2000**, *210*, 251. (c) Gaspar, P. P.; West, R. In *The Chemistry of Organic Silicon Compounds*; Rappoport, Z., Apeloig, Y., Eds.; Wiley: Chichester, U.K., 1998; Vol. 2, Part 3, Chapter 43.
(14) Bergner, A.; Dolg, M.; Kuechle, W.; Stoll, H.; Preuss, H. *Mol. Phys.* **1993**, *80*, 1431.
(15) Based on a comparison between the ΔE_{S-T} values of H$_2$Sn**:** and Me$_2$Sn**:** calculated by us at the B3LYP/SDD level of theory and the corresponding values calculated previously[17,18] at the higher MCSCF and CCSD(T) levels of theory.
(16) Holthausen, M. C.; Koch, W.; Apeloig, Y. *J. Am. Chem. Soc.* **1999**, *121*, 2623.
(17) (a) Balasubramanian, K. *J. Chem. Phys.* **1988**, *89*, 5731. (b) Matsunaga, N.; Koseki, S.; Gordon, M. S. *J. Chem. Phys.* **1996**, *104*, 7988.
(18) Su, M.-D. *Chem.−Eur. J.* **2004**, *10*, 6073.

Table 2. Comparison of RR′Sn═SnRR′ Distannene Structures

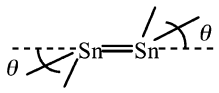

Trans-Bent Angle θ

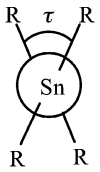

Twisting Angle τ

R, R′	R = R′ = ^{t}Bu$_2$MeSi[a]	R = (Me$_3$Si)$_3$Si R′ = Ar[b]	R = R′ = (Me$_3$Si)$_2$CH[c]	R = (Me$_3$Si)$_3$Si R′ = Ar[d]	R = R′ = (Me$_3$Si)$_3$Si[e]	R = (Me$_3$Si)$_3$Si R′ = Ar[f]
Sn═Sn (Å)	2.6683(10)	2.702	2.768(1)	2.7914(4)	2.8247(6)	2.833(1)
sum of bond angles around Sn atoms (deg)	359.98	not available	343.5	337.4	351.96	337.9
trans-bent angle θ (deg)	1.22(5)	39.4	41.0	44.9	28.6	41.5
Sn═Sn geometry	nonbent	*trans*-bent	*trans*-bent	*trans*-bent	*trans*-bent	*trans*-bent
twisting angle τ (deg)	44.62(7)	0	0	0	63.2	0
color	dark green	not available	brick red	brown-violet	black	violet-red

[a] This work. [b] Ar = 2,4,6-Me$_3$-C$_6$H$_2$, ref 8b. [c] Reference 8a. [d] Ar = 2-^{t}Bu-4,5,6-Me$_3$-C$_6$H, ref 8c. [e] Reference 8d. [f] Ar = 2,4,6-(CF$_3$)$_3$-C$_6$H$_2$, ref 8e.

Scheme 2

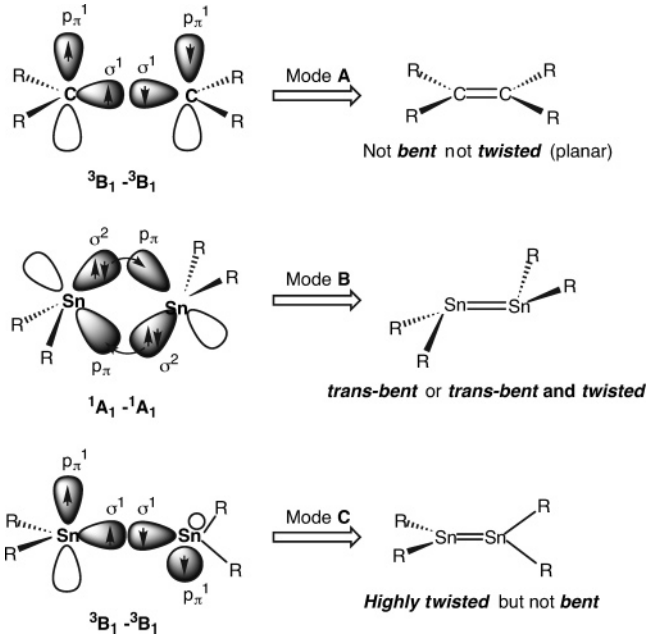

available examples of ^{119}Sn NMR spectra of distannenes measured at room temperature in solution: +427.3 ppm (for tetrakis(2,4,6-triisopropylphenyl)distannene)[19] and +412 ppm (for cyclotristannene).[20] As was discussed above, distannenes R$_2$Sn═SnR$_2$ typically tend to dissociate in solution into a pair of the corresponding stannylenes R$_2$Sn**:**, which was clearly manifested by their diagnostic downfield shifted resonances of the ^{119}Sn NMR chemical shifts.[3f,g] The only distannene that preserves its Sn═Sn double bond undissociated in solution at room temperature was cyclotristannene, reported recently by Wiberg.[20] However, this compound has a specific structure whose properties are greatly affected by its unique cyclic skeleton. Thus, our distannene **1** represents the first example of a Sn═Sn double bond in the isolable acyclic distannenes that is stable in solution at room temperature and even upon heating.[21]

UV Spectrum of 1. It is interesting that distannene **1** has a rather unusual dark-green color. Accordingly, the longest wavelength absorption maximum in the UV spectrum of **1** was observed at 670 nm, whose position did not change in the temperature interval from 273 to 203 K. This absorption is greatly red-shifted compared with that of Tip$_2$Sn═SnTip$_2$ (Tip = 2,4,6-triisopropylphenyl), the only distannene relatively stable in solution at low temperature, which has a red color and absorption maximum λ_{max} = 494 nm (−70 °C).[19] There are several reasons which may contribute to such an experimental observation of the bathochromic shift of **1**, which all originate from the high twisting of the Sn═Sn double bond substituted by the electropositive σ-donating silyl groups. The first one is the possibility of the 5p$_\pi$(Sn)−σ(Sn−Si) orbitals mixing, raising the energy of the HOMO level and, consequently, decreasing the HOMO−LUMO energy gap of **1**. Such an 5p$_\pi$(Sn)−σ(Sn−Si) interaction of orbitals might be possible upon the experimentally observed twisting of the Sn═Sn double bond in **1**. Another important reason of the bathochromic shift is the reduced overlap of the two 5p$_\pi$(Sn) orbitals upon the twisting of the Sn═Sn double bond, which should also lead to the destabilization of the HOMO. To gain further insight into the electronic structure of distannene **1** we have performed theoretical calculations on the model compound (Me$_3$Si)$_2$Sn═Sn(SiMe$_3$)$_2$ (Figure 2).[9] Geometry optimization provided us a *trans*-bent (bend angle 32.5°) very slightly twisted (twist angle 3.7°) conformation **A** as a minimum structure (Figure 2, **A**). The discrepancy between the experimental (nonpyramidal, highly twisted) and calculated (*trans*-bent, very slightly twisted) geometries of distannene could be attributed to the different substitution patterns at the Si atoms (Me$_3$Si in calculated model vs much more bulky ^{t}Bu$_2$MeSi in the real compound **1**). Inspection of the MOs revealed that in the slightly twisted structure **A** the HOMO (−4.54 eV) and LUMO (−2.07 eV) energy gap is rather small (ΔE = 2.47 eV), thus making HOMO−LUMO promotion easily accessible (Figure 2, **A**). Then we performed single-point energy calculations based on

(19) Masamune, S.; Sita, L. R. *J. Am. Chem. Soc.* **1985**, *107*, 6390.
(20) Wiberg, N.; Lerner, H.-W.; Vasisht, S.-K.; Wagner, S.; Karaghiosoff, K.; Nöth, H.; Ponikwar, W. *Eur. J. Inorg. Chem.* **1999**, 1211.
(21) The only examples of heavy alkene analogues containing sp^2-Sn atoms, which are stable both in the solid state and in solution, were recently synthesized by us: silastannene >Si═Sn< (see ref 2j) and germastannenes >Ge═Sn< (see ref 2*l*,m). The example of the transient distannene, Me$_2$Sn═SnMe$_2$, which does not dissociate in solution, was also recently reported: Becerra, R.; Gaspar, P. P.; Harrington, C. R.; Leigh, W. J.; Vargas-Baca, I.; Walsh, R.; Zhou, D. *J. Am. Chem. Soc.* **2005**, *127*, 17469.

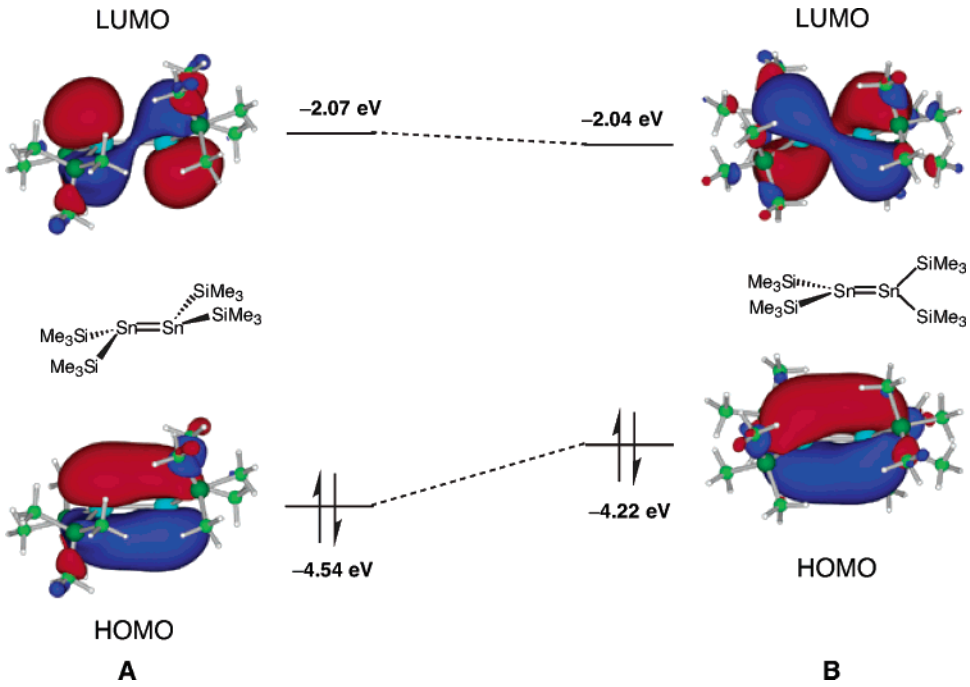

Figure 2. Molecular orbitals of the model $(Me_3Si)_2Sn{=}Sn(SiMe_3)_2$ distannene: (A) *trans*-bent, nontwisted conformation; (B) nonbent, highly twisted conformation.

the X-ray structure of **1** to verify the properties of the highly twisted geometry of the Sn═Sn double bond in conformation **B** (Figure 2, **B**). It was found that upon twisting the Sn═Sn double bond on going from structure **A** to structure **B** the energy of the HOMO level increased to −4.22 eV, whereas the energy of the LUMO level remained almost unchanged (−2.04 eV). In the twisted structure **B** the HOMO is the $5p_\pi{-}5p_\pi$ (Sn═Sn) orbital with a contribution of σ(Sn−Si) orbitals (Figure 2, **B**). In effect, the HOMO−LUMO gap decreased upon twisting the Sn═Sn double bond to 2.18 eV (in **B**) vs 2.47 eV (in **A**). In total, these calculation results provide some theoretical explanation to the experimentally observed bathochromic shift in the UV spectrum of distannene **1**.

Finally, the manifestation of the double bond between the Sn atoms was also clearly demonstrated by the characteristic reactivity of distannene **1**, which will be discussed in the following section.

Reactivity of 1. Because all previously known distannenes dissociate in solution into the corresponding stannylenes, the reactivity of distannenes described thus far was, in fact, the reactivity of >Sn**:** species rather than the Sn═Sn double bond.[3f,g] Below, we will present the first convincing examples of the reactivity of the Sn═Sn double bond of distannene **1**.

Reaction of 1 with Carbon Tetrachloride. It is now well established that the halogenation of the disilenes $R_2Si{=}SiR_2$ and digermenes $R_2Ge{=}GeR_2$ with simple alkyl halides such as CCl_4 results in the formation of the stable 1,2-dichlorodisilanes $R_2(Cl)Si{-}Si(Cl)R_2$[22a] and -digermanes $R_2(Cl)Ge{-}Ge(Cl)R_2$.[22b] However, the reaction of distannene $Dis_2Sn{=}SnDis_2$ (Dis = $CH(SiMe_3)_2$) with either CCl_4 or Cl_2 gave only 1,1-dichlorostannane R_2SnCl_2 as the final compound, which can be considered as the chlorinated product of stannylenes R_2Sn**:** formed upon the dissociation of the $R_2Sn{=}SnR_2$ double bond.[23]

Scheme 3

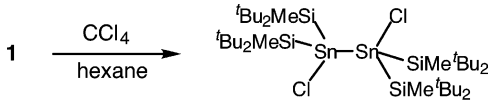

3

Our distannene **1** reacts with carbon tetrachloride with an immediate color change from dark green to pale yellow. The product, 1,2-dichloro-1,1,2,2-tetrakis(di-*tert*-butylmethylsilyl)-distannane **3**, was isolated by recrystallization from hexane as pale-yellow crystals in 75% yield (Scheme 3). The ^{1}H NMR spectrum of **3** exhibited the two distinct resonances of diastereotopic ^{t}Bu groups, which is expected for 1,2-dichloride $(^tBu_2MeSi)_2(Cl)Sn{-}Sn(Cl)(SiMe^tBu_2)_2$ but not for 1,1-dichloride $(^tBu_2MeSi)_2SnCl_2$. The structure of **3** was undoubtedly established by the X-ray crystallographic analysis. However, we do not discuss the structural details because of the unsatisfactory refinement.

Reaction of 1 with Phenylacetylene. The [2 + 2] cycloaddition of the simple acetylenes across the >E═E< bonds of heavy alkenes is a powerful tool in elucidating the nature of the double bond. In the case of disilenes and digermenes, the 1,2-disila- and 1,2-digermacyclobut-3-enes are the anticipated and virtual products of these reactions.[22c,d] In the case of distannenes, formation of the four-membered [2 + 2] cycloadduct competes with formation of the three-membered [1 + 2] cycloadduct due to the intrinsic distannene−stannylene equilibrium in solution (Scheme 4).

Distannene **1** smoothly reacted with an excess of phenylacetylene to produce immediately the [2 + 2] cycloaddition

(22) (a) Kira, M.; Iwamoto, T. *J. Organomet. Chem.* **2000**, *611*, 236. (b) According to our experimental data, tetrasilyl-substituted digermenes smoothly react with CCl_4 to form the corresponding 1,2-dichlorodigermanes without breaking the central Ge−Ge bond. These data will be published in forthcoming papers. (c) Okazaki, R.; West. R. *Adv. Organomet. Chem.* **1996**, *39*, 231. (d) Escudié, J.; Ranaivonjatovo, H. *Adv. Organomet. Chem.* **1999**, *44*, 113.

(23) Cotton, J. D.; Davidson, P. J.; Lappert, M. F. *J. Chem. Soc., Dalton Trans.* **1976**, 2275.

Scheme 4

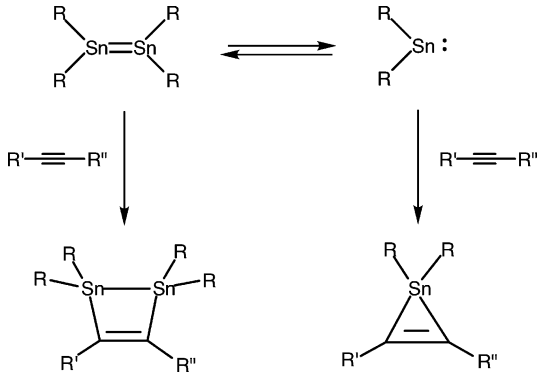

Scheme 5

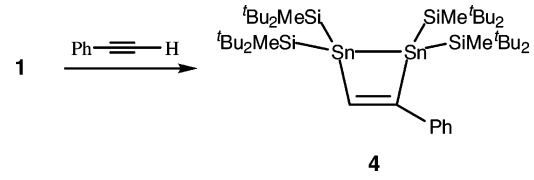

4

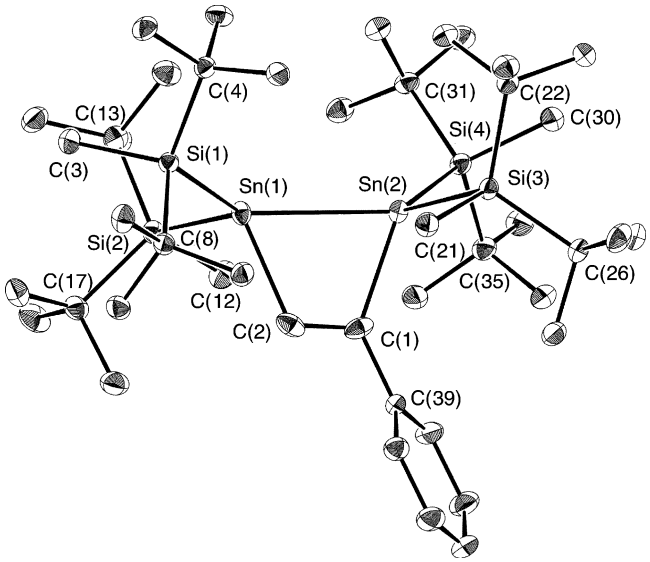

Figure 3. Crystal structure of **4** (ORTEP plot; thermal ellipsoids are shown at the 30% probability; hydrogen atoms are omitted). The position of the Ph group is disordered between the C(1) and C(2) atoms, and the major contribution (78% probability) is shown.

product, 1,1,2,2-tetrakis(di-*tert*-butylmethylsilyl)-3-phenyl-1,2-distannacyclobut-3-ene **4**, isolated by recrystallization from hexane as yellow plates in 64% yield (Scheme 5). The structure of **4** was elucidated on the basis of NMR spectral data and X-ray crystallography (Figure 3, Table 3).

In the ^{119}Sn NMR spectrum of **4** the two signals of the skeletal Sn atoms were observed at −329.6 and −175.7 ppm ($^1J(^{119}\text{Sn}-^{119,117}\text{Sn}) = 1354$ Hz). Such a coupling constant is smaller than those of the similar [2 + 2] cycloadducts of phenylacetylene with other distannenes ($^1J(^{119}\text{Sn}-^{119,117}\text{Sn})$ ranging from 2436 to 4462 Hz).[24] This gives evidence for the longer Sn−Sn bond separation in **4** compared with other similar [2 + 2] cycloadducts.

Table 3. Selected Bond Lengths (Å) and Angles (deg) of **4**[a]

Bond Length			
Sn(1)−Sn(2)	2.9004(3)	Si(1)−C(8)	1.932(2)
Sn(1)−C(2)	2.188(3)	Si(2)−C(12)	1.891(3)
Sn(1)−Si(1)	2.6496(7)	Si(2)−C(13)	1.936(3)
Sn(1)−Si(2)	2.6400(7)	Si(2)−C(17)	1.930(3)
Sn(2)−C(1)	2.228(3)	Si(3)−C(21)	1.884(3)
Sn(2)−Si(3)	2.6581(7)	Si(3)−C(22)	1.939(3)
Sn(2)−Si(4)	2.6709(7)	Si(3)−C(26)	1.935(3)
C(1)−C(2)	1.327(4)	Si(4)−C(30)	1.886(3)
Si(1)−C(3)	1.884(3)	Si(4)−C(31)	1.934(3)
Si(1)−C(4)	1.925(3)	Si(4)−C(35)	1.924(3)
		C(1)−C(39)	1.498(4)
Bond Angle			
C(2)−Sn(1)−Sn(2)	68.95(8)	C(2)−Sn(1)−Si(2)	99.81(7)
Sn(1)−Sn(2)−C(1)	68.88(8)	Sn(1)−Sn(2)−Si(3)	111.377(16)
Sn(2)−C(1)−C(2)	108.9(2)	Sn(1)−Sn(2)−Si(4)	129.427(18)
C(1)−C(2)−Sn(1)	111.9(2)	C(1)−Sn(2)−Si(3)	101.17(7)
Sn(2)−Sn(1)−Si(1)	133.324(17)	C(1)−Sn(2)−Si(4)	125.19(8)
Sn(2)−Sn(1)−Si(2)	110.420(18)	Si(3)−Sn(2)−Si(4)	111.85(2)
Si(1)−Sn(1)−Si(2)	113.47(2)	Sn(2)−C(1)−C(39)	134.9(2)
C(2)−Sn(1)−Si(1)	116.98(8)	C(2)−C(1)−C(39)	115.2(3)

[a] Atomic numbers are given in Figure 3. Standard deviations are in parentheses.

The X-ray analysis of **4** clearly confirms its 1,2-distannacyclobut-3-ene composition. The four-membered ring of **4** is nearly planar with the sum of the internal bond angles being 358.63°, similar to other 1,2-distannacyclobut-3-enes.[24] The Sn−Sn bond in **4** of 2.9004(3) Å is significantly longer than the average Sn−Sn single bond of ca. 2.81 Å[10] and Sn−Sn distances in other known 1,2-distannacyclobut-3-enes (2.817(1)[24a] and 2.840(1) Å),[24b] which can be ascribed to the high steric demand of the bulky ^{t}Bu$_2$MeSi groups on the Sn atoms.

One-Electron Reduction of 1. The heavy analogues of alkenes of the type >E═E< (E = Si, Ge, Sn, and Pb) are expected to be reduced more smoothly than the corresponding alkenes >C═C< because of the low-lying and easily accessible LUMOs of the former compared with those of the latter. However, to date the generation of only disilene anion radicals has been reported in the scientific literature. Thus, Weidenbruch reported in 1985 the generation of the first representatives of disilene anion radicals $[R_2Si{=}SiR_2]^{\bullet-}$ (R = ^{i}Pr, ^{t}Bu) by the reduction of 1,2-dihalodisilanes $R_2(X)Si{-}Si(X)R_2$ with alkali metals in THF.[25] Such anion radical species with a lifetime of several minutes at room temperature exhibited an EPR spectrum with hyperfine coupling constant (hfcc) $a(^{29}\text{Si}) = 3.36$ mT. Following this original report, Kira commented on the generation of disilene anion radicals by the direct reduction of stable tetrasilyldisilenes with potassium in DME.[22a] And finally, the first virtually stable disilene anion radical was synthesized and structurally characterized by the reduction of the disilene (^{t}Bu$_2$MeSi)$_2$Si═Si(SiMe^{t}Bu$_2$)$_2$ with ^{t}BuLi in THF.[26]

The reduction of distannene **1** was achieved by its treatment with an equivalent amount of potassium mirror in THF in the presence of [2.2.2]cryptand to produce the first and still only example of a distannene anion radical (Scheme 6). The tetrakis(di-*tert*-butylmethylsilyl)distannene anion radical **5** was isolated as a dark-red solid in 82% yield. The crystal structure of **5** is represented by the highly twisted (twist angle 74°) Sn−Sn

(24) (a) Sita, L. R.; Kinoshita, I.; Lee, S. P. *Organometallics* **1990**, *9*, 1644. (b) Weidenbruch, M.; Schäfer, A.; Kilian, H.; Pohl, S.; Saak, W.; Marsmann, H. *Chem. Ber.* **1992**, *125*, 563.
(25) Weidenbruch, M.; Kramer, K.; Schäfer, A.; Blum, J. K. *Chem. Ber.* **1985**, *118*, 107.
(26) Sekiguchi, A.; Inoue, I.; Ichinohe, M.; Arai, Y. *J. Am. Chem. Soc.* **2004**, *126*, 9626.

Scheme 6

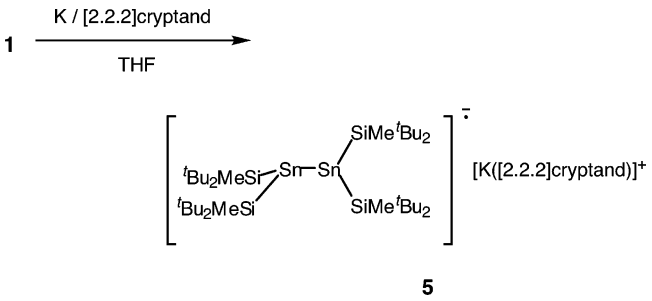

skeleton with a Sn−Sn bond length of 2.8978(3) Å, which is 0.2295 Å longer than that of the starting distannene **1** due to the decrease in bond order upon one-electron reduction of the double bond (Figure 4, Table 4). The geometry around the two Sn atoms is different: one of them is essentially planar (sum of the bond angles 355.39°, *trans*-bend angle 19.50(4)°) as a radical center, whereas the other one is profoundly pyramidal (sum of the bond angles 323.16°, *trans*-bend angle 60.05(4)°) being an anionic center. The characteristic planarity of the silyl-substituted stannyl radicals (for example, $(^t\text{Bu}_2\text{MeSi})_3\text{Sn}^\bullet$)[7] and pyramidalization of the silyl-substituted stannyl anions (for example, $(^t\text{Bu}_2\text{MeSi})_3\text{Sn}^-$)[27] was established in our previous studies. This implies that the negative charge and the unpaired electron are effectively separated between the two Sn atoms in distannene anion radical **5**. It is interesting that such charge-electron separation is also maintained in the solution of the distannene anion radical. This was manifested in the EPR spectrum of **5** exhibiting a single resonance ($g = 2.0517$) with two distinct pairs of satellite signals with hfcc values of 34.0 mT (α-^{119,117}Sn) and 18.7 mT (β-^{119,117}Sn), respectively, implying localization of the unpaired electron on one of the two Sn atoms. In marked contrast, in disilene anion radical $[(^t\text{Bu}_2\text{MeSi})_2\text{Si}-\text{Si}(\text{SiMe}^t\text{Bu}_2)_2]^{\bullet-}$ the unpaired electron is quickly exchanged between both skeletal silicon atoms on the EPR time scale, which, however, can be suppressed at low temperature (120 K).[26]

The EPR spectra of the distannene anion radical were also measured in 2-methyl-THF at glass matrix conditions (100 K). Expectedly, the low symmetry of the distannene anion radical caused the three-axis anisotropy of the *g*-factor of **5**, in which the contributors were determined as $g_{xx} = 2.109$, $g_{yy} = 2.057$, and $g_{zz} = 1.988$ (Figure 5a).

Most importantly, at high concentration and high gain, a very characteristic single resonance (1631 G) corresponding to a forbidden $\Delta M_s = 2$ electronic transition was observed at a field strength approximately half of the center of the allowed $\Delta M_s = 1$ electronic transition (the so-called *half-field* region).[28] Such $\Delta M_s = 2$ transitions are intrinsically less anisotropic than the $\Delta M_s = 1$ transitions, and therefore only a single broad signal is typically observed. It is known that such $\Delta M_s = 2$ forbidden transitions are characteristic for randomly oriented triplet systems being the result of the magnetic interaction between the two parallel spins.[28] The spin−spin dipolar interaction in triplet biradicals leads to the fine structure of the EPR spectrum, and three pairs of sidelines are expected to appear ($\Delta M_s = 1$ transition).[29] However, in the EPR spectrum of **5** the species with spin $S = {}^1/_2$ dominate, which does not allow the observation of sidelines and determination of the zero-field splitting parameters $|D'|$ and $|E'|$ for interaction between the two electrons in paramagnetic species having spin $S = 1$. We can estimate $|D'|$ from the fact that the total width of the EPR spectrum signals of **5** occupies a range of ~200 G; that is, the $2|D'|$ value cannot exceed 200 G, or otherwise sidelines could be observed. Assuming the spin−spin dipolar interactions, $|D'|$ is approximately given by the equation $|D'| = {}^3/_2 g^2 b^2 r^{-3}$, where *g* is the *g*-factor value, *r* is the distance between the two interacting electrons, and *b* is the Bohr magneton.[29] If $|D'| = 100$ G, the minimum distance between the two electrons in the triplet species can be estimated as 5.3 Å. Therefore, in our case there is evidence that the distance between the two interacting electrons in the triplet species is greater than 5.3 Å, but on the other hand this distance should be shorter than 12 Å ($|D'| < 8$ G), the maximum distance at which the signal in the *half-field* region is detectable by the X-band EPR spectrometer.

One can suggest that the molecules of distannene anion radical **5** can partially aggregate at low temperature to form paramagnetic triplet dimers **6** (Scheme 7) through the coordination of the anionic Sn center of one molecule of **5** to the potassium countercation of another molecule of **5**.

The low-temperature aggregation of anion radicals of similar type, involving participation of countercations and solvent molecules, was previously observed for paramagnetic ketyl dimers, though it was found to be a minor process in strongly solvating solvents such as DMF.[28a] To compare the low-temperature EPR data of **5**, we have measured the EPR spectrum of the previously synthesized neutral stannyl radical $(^t\text{Bu}_2\text{MeSi})_3\text{Sn}^\bullet$[7] **2** at the same conditions (2-Me-THF, 100 K). The EPR spectrum of **2** is typical for a system with axial symmetry, the *g*-factor being characterized by the two components $g_\perp = 2.074$ and $g_{II} = 1.993$ (Figure 5b). In this case the signal in the *half-field* region corresponding to a forbidden $\Delta M_s = 2$ transition was not observed, in contrast to the above case of distannene anion radical **5**, because such a type of paramagnetic aggregation of the neutral radicals **2**, lacking the anionic center, is unlikely.

Experimental Section

General Procedures. All manipulations with the air-sensitive compounds were carried out using an MBRAUN MB 150B-G glovebox, a high-vacuum line and Schlenk techniques, and dry, oxygen-free solvents. NMR spectra were recorded on Bruker AC-300FT (^{1}H NMR at 300.13 MHz; ^{13}C NMR at 75.47 MHz; ^{29}Si NMR at 59.63 MHz; ^{119}Sn NMR at 111.92 MHz) and ARX-400FT NMR spectrometers (^{1}H NMR at 400.23 MHz; ^{13}C NMR at 100.65 MHz; ^{29}Si NMR at 79.51 MHz; ^{119}Sn NMR at 149.32 MHz). The EPR spectra were measured on a Bruker EMX-T EPR spectrometer, UV−vis and mass spectra were recorded on SHIMADZU UV-3150 and JEOL JMS-SX102A spectrometers, respectively. Starting materials $SnCl_2$-diox[30] and ^{t}Bu$_2$MeSiNa[31] were synthesized according to the previously reported experimental procedures.

(27) Fukawa, T.; Nakamoto, M.; Lee, V. Ya.; Sekiguchi, A. *Organometallics* **2004**, *23*, 2376.
(28) For the discussion concerning the nature of *half-field* EPR signals, corresponding to a forbidden $\Delta M_s = 2$ electronic transition, see: (a) Hirota, N.; Weissman, S. I. *J. Am. Chem. Soc.* **1964**, *86*, 2538. (b) Hirota, N. *J. Am. Chem. Soc.* **1967**, *89*, 32. (c) Takeshita, T.; Hirota, N. *J. Am. Chem. Soc.* **1971**, *93*, 6421. (d) Jain, R.; Sponsler, M. B.; Coms, F. D.; Dougherty, D. A. *J. Am. Chem. Soc.* **1988**, *110*, 1356.
(29) Wertz, J.; Bolton, J. *Electron Spin Resonance*; McGraw-Hill: New York, USA, 1972; Chapter 10.
(30) Hough, E.; Nicholson, D. G. *J. Chem. Soc., Dalton Trans.* **1976**, 1782.
(31) Sekiguchi, A.; Fukawa, T.; Nakamoto, M.; Lee, V. Ya.; Ichinohe, M. *J. Am. Chem. Soc.* **2002**, *124*, 9865.

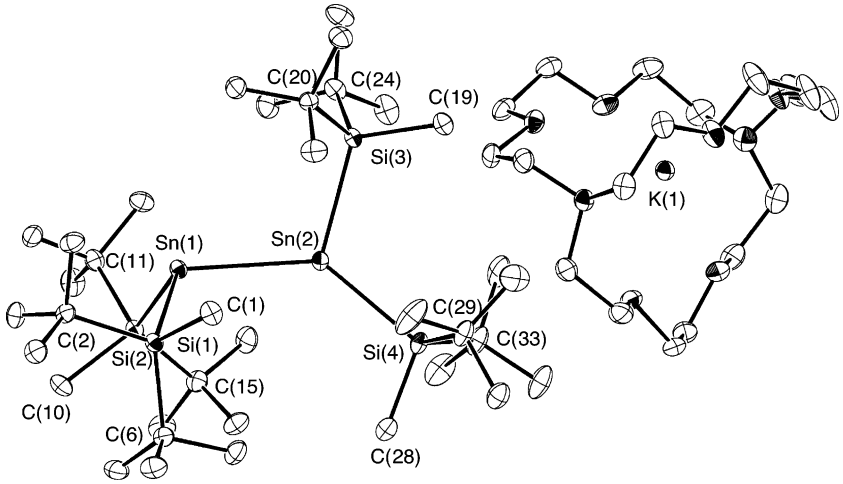

Figure 4. Crystal structure of **5** (ORTEP plot; thermal ellipsoids are shown at the 30% probability; hydrogen atoms are omitted).

Table 4. Selected Bond Lengths (Å) and Angles (deg) of **5**[a]

Bond Length			
Sn(1)−Sn(2)	2.8978(3)	Sn(2)−Si(3)	2.6432(9)
Sn(1)−Si(1)	2.6679(8)	Sn(2)−Si(4)	2.6507(9)
Sn(1)−Si(2)	2.6781(8)	Si(3)−C(19)	1.890(3)
Si(1)−C(1)	1.901(3)	Si(3)−C(20)	1.943(3)
Si(1)−C(2)	1.954(3)	Si(3)−C(24)	1.937(3)
Si(1)−C(6)	1.949(3)	Si(4)−C(28)	1.891(4)
Si(2)−C(10)	1.900(3)	Si(4)−C(29)	1.937(4)
Si(2)−C(11)	1.946(3)	Si(4)−C(33)	1.924(3)
Si(2)−C(15)	1.937(3)		
Bond Angle			
Sn(2)−Sn(1)−Si(1)	107.51(2)	Sn(1)−Sn(2)−Si(3)	107.34(2)
Sn(2)−Sn(1)−Si(2)	105.836(19)	Sn(1)−Sn(2)−Si(4)	134.39(2)
Si(1)−Sn(1)−Si(2)	109.81(3)	Si(3)−Sn(2)−Si(4)	113.66(3)
Sn(1)−Si(1)−C(1)	106.99(11)	Sn(2)−Si(3)−C(19)	114.48(11)
Sn(1)−Si(1)−C(2)	102.63(10)	Sn(2)−Si(3)−C(20)	110.72(10)
Sn(1)−Si(1)−C(6)	124.52(10)	Sn(2)−Si(3)−C(24)	109.69(11)
Sn(1)−Si(2)−C(10)	113.34(10)	Sn(2)−Si(4)−C(28)	109.65(12)
Sn(1)−Si(2)−C(11)	104.61(10)	Sn(2)−Si(4)−C(29)	114.15(11)
Sn(1)−Si(2)−C(15)	118.14(11)	Sn(2)−Si(4)−C(33)	110.15(11)

[a] Atomic numbers are given in Figure 4. Standard deviations are in parentheses.

Synthesis of Tetrakis(di-*tert*-butylmethylsilyl)distannene 1. Dry THF (30 mL) was vacuum transferred to a mixture of $SnCl_2$-diox (924 mg, 3.33 mmol) and $^tBu_2MeSiNa$ (1.5 g, 8.32 mmol). The reaction mixture was initially stirred at −78 °C and then overnight with gradual warming to room temperature to produce a dark-green solution. After removal of inorganic salt and polymeric materials, the solvent was evaporated in a vacuum. The dark-green residue was recrystallized from hexane at −30 °C to give distannene as dark-green crystals (620 mg, 43%): mp 172−174 °C (dec); ^{1}H NMR (C_6D_6, δ) 0.83 (s, 12 H, CH_3), 1.34 (s, 72 H, $(CH_3)_3C$); ^{13}C NMR (C_6D_6, δ) 4.6 (CH_3), 32.3 ($(CH_3)_3C$), 36.4 ($(CH_3)_3C$); ^{29}Si NMR (C_6D_6, δ) 46.9; ^{119}Sn NMR (C_6D_6, δ) 630.7; UV−vis (hexane) λ_{max}/nm (ϵ): 309 (8300), 395 (4200), 670 (3100). Anal. Calcd for $C_{36}H_{84}Si_4Sn_2$: C, 49.88; H, 9.77. Found: C, 49.59; H, 9.65.

Synthesis of 1,2-Dichloro-1,1,2,2-tetrakis(di-*tert*-butylmethylsilyl)-distannane 3. Dry CCl_4 (1 mL) was vacuum transferred to distannene **1** (63 mg, 0.073 mmol), and then the reaction mixture was stirred for 5 min at room temperature. Excess CCl_4 was evaporated in a vacuum to give **3** as pale-yellow crystals (51 mg, 75%): mp 147−148 °C (dec); ^{1}H NMR (C_6D_6, δ) 0.74 (s, 12 H, CH_3), 1.24 (s, 36 H, $(CH_3)_3C$), 1.26 (s, 36 H, $(CH_3)_3C$); ^{13}C NMR (C_6D_6, δ) −2.2 (CH_3), 23.0 ($(CH_3)_3C$), 24.3 ($(CH_3)_3C$), 29.5 ($(CH_3)_3C$), 29.9 ($(CH_3)_3C$); ^{29}Si NMR (C_6D_6, δ) 44.8; ^{119}Sn NMR (C_6D_6, δ) 59.1; UV−vis (hexane) λ_{max}/nm (ϵ): 271 (54 600), 318 (46 200); Anal. Calcd for $C_{36}H_{84}Cl_2Si_4Sn_2$: C, 46.11; H, 9.03. Found: C, 46.10; H, 8.92.

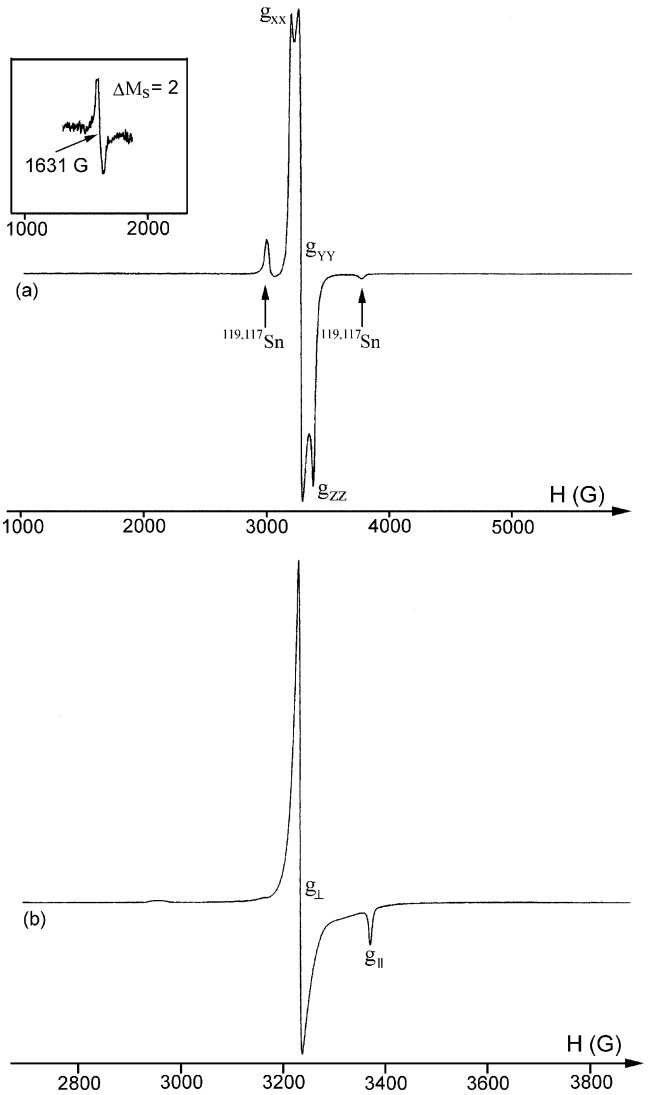

Figure 5. (a) The EPR spectrum of anion radical **5** in 2-methyl-THF at 100 K. The insert shows the resonance corresponding to a forbidden $\Delta M_s = 2$ transition. (b) The EPR spectrum of neutral stannyl radical ($^tBu_2MeSi)_3Sn^\bullet$ in 2-methyl-THF at 100 K.

Synthesis of 1,2-Tetrakis(di-*tert*-butylmethylsilyl)-3-phenyl-1,2-distannacyclobut-3-ene 4. Phenylacetylene (0.5 mL, 4.55 mmol) was vacuum transferred to a benzene solution (1 mL) of distannene **1** (90 mg, 0.104 mmol). The solution color gradually changed from dark green

Scheme 7

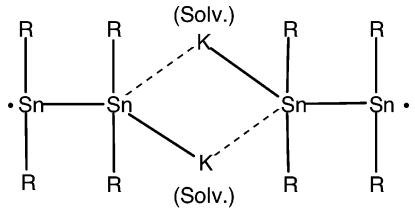

6, R = SiMe^{t}Bu$_2$

to reddish purple. After 3 h of stirring, solvent and excess phenylacetylene were evaporated in a vacuum. The residue was recrystallized from hexane to give **4** as yellow crystals (68 mg, 64%): mp 184−187 °C; ^{1}H NMR (C_6D_6, δ) 0.70 (s, 6 H, CH_3), 0.74 (s, 6 H, CH_3), 1.10 (s, 18 H, $(CH_3)_3C$), 1.16 (s, 18 H, $(CH_3)_3C$), 1.26 (s, 18 H, $(CH_3)_3C$), 1.27 (s, 18 H, $(CH_3)_3C$), 7.00 (t, J = 7.3 Hz, 1 H, H_{para}), 7.15 (t, J = 7.3 Hz, 2 H, H_{meta}), 7.43 (d, J = 7.3 Hz, 2 H, H_{ortho}), 8.43 (s, 1 H, CPh═C*H*); ^{13}C NMR (C_6D_6, δ) 0.6 (CH_3), 0.7 (CH_3), 23.0 ($(CH_3)_3C$), 23.3-($(CH_3)_3C$), 23.9 (2 C, $(CH_3)_3C$)), 30.8 (($CH_3)_3$C), 31.0 (($CH_3)_3$C), 31.3 (($CH_3)_3$C), 31.6 (($CH_3)_3$C), 126.2 (C_{arom}), 127.4 (C_{arom}), 128.1 (C_{arom}), 149.4 (C_{ipso}), 154.0 (PhC═*C*H), 169.3 (Ph*C*═CH); ^{29}Si NMR (C_6D_6, δ) 30.2, 31.3; ^{119}Sn NMR (C_6D_6, δ) −330.0, −176.1; UV−vis (hexane) λ_{max}/nm (ϵ): 220 (51 500), 286 (15 600), 316 (15 200). Anal. Calcd for $C_{44}H_{92}Si_4Sn_2$: C, 54.43; H, 9.55. Found: C, 54.37; H, 9.35.

Synthesis of Tetrakis(di-*tert*-butylmethylsilyl)distannene Anion-Radical 5. Dry THF (2 mL) was vacuum transferred to a mixture of distannene **1** (300 mg, 0.346 mmol) and [2.2.2]cryptand (140 mg, 0.345 mmol). Then the resulting solution was shortly contacted to potassium mirror (14 mg, 0.358 mmol), and the color of solution immediately changed from dark green to dark red. Solvent was evaporated in a vacuum, and the residue was washed with dry hexane in a glovebox to give distannene anion radical **5** as a dark-red powder (375 mg, 82%): EPR (2-Me-THF, 298 K) g = 2.0517, hfccs a(α-^{119,117}Sn) = 34.0 mT, a(β-^{119,117}Sn) = 18.7 mT.

X-ray Crystal Structure Analyses. Single crystals suitable for an X-ray diffraction study were grown from the following solvents: **1** and **5** from toluene; **4** from hexane. Diffraction data were collected on a Mac Science DIP2030K image plate diffractometer employing graphite-monochromatized Mo Kα radiation (λ = 0.710 70 Å). The structures were solved by direct method and refined by the full-matrix least-squares method using an SHELXL-97 program. Crystal data for **4** at 120 K: MF = $C_{44}H_{90}Si_4Sn_2$, MW = 968.90, triclinic, $P\bar{1}$, a = 11.7250(3) Å, b = 13.0250(6) Å, c = 18.7090(8) Å, α = 75.877(2)°, β = 87.714(3)°, γ = 68.845(4) °, V = 2580.44(18) Å^3, Z = 2, D_{calcd} = 1.247 g·cm^{-3}. The final R factor was 0.0335 for 9339 reflections with $I > 2\sigma(I)$ (Rw = 0.0914 for all data, 25 788 reflections), GOF = 1.034. For the detailed information of the X-ray structure determination for **1** and **5**, see the Supporting Information in ref 7.

Acknowledgment. This work was supported by Grants-in-Aid for Scientific Research (Research Nos. 16205008, 17550029, 17750031, 17655014, 18037008, 18039004) from the Ministry of Education, Science and Culture of Japan, JSPS Research Fellowship for Young Scientists (T.F.), COE (Center of Excellence) program, Israel Science Foundation administrated by Israel Academy of Sciences and Humanities, Fund for the Promotion of Research at the Technion, and Minerva Foundation in Munich. B.T. is grateful for support to the Center for Absorption in Science, Israel Ministry of Immigrant Absorption, State of Israel.

Supporting Information Available: Tables giving the details of the X-ray structure determination, thermal ellipsoid plots, fractional atomic coordinates, anisotropic thermal parameters, bond lengths, and bond angles for **4** (PDF and CIF), complete ref 9. This material is available free of charge via the Internet at http://pubs.acs.org.

JA063322X